Over-representation of MEF-2 isoforms (A/C) is associated with HTLV-1-induced acute ATLL and their recruitment to 3'LTR facilitates HBZ expression from the antisense promoter via interactions with Menin and Jun D

Kiran Madugula
Drexel University College of Medicine
Julie Joseph
Drexel University College of Medicine
Vanessa Teixeira
Instituto de Ciencias Biológicas: Instituto de Ciencias Biologicas
Rashida Ginwala
Fox Chase Cancer Center
Catherine Demarino
George Mason University
Fatah Kashanchi
George Mason University
Amanda Rushing
East Carolina University Brody School of Medicine
Isabelle Lemasson
East Carolina University Brody School of Medicine
Sydney Wilson
Drexel University College of Medicine
Dominc Sales
Drexel University College of Medicine
Edward Harhaj
Penn State: The Pennsylvania State University
Murali Janakiram
Albert Einstein Medical Center
B. Hilda Ye
Albert Einstein Medical Center
Zafar K Khan
Drexel University College of Medicine

Pooja Jain (pj27@drexel.edu)
Drexel University College of Medicine https://orcid.org/0000-0002-9925-4259

Research Article

Keywords: HTLV-1, ATLL, Myocyte Enhancer Factor, MEF-2A, MEF-2C, Menin, Jun D

Posted Date: April 3rd, 2021

DOI: https://doi.org/10.21203/rs.3.rs-362537/v1

Over-representation of MEF-2 isoforms (A/C) is associated with HTLV-1-induced acute ATLL and their recruitment to 3'LTR facilitates HBZ expression from the antisense promoter via interactions with Menin and Jun D

Kiran K. Madugula[1], Julie Joseph[1], Vanessa Teixeira[1,2], Rashida Ginwala[1], Catherine Demarino[3], Fatah Kashanchi[3], Amanda W. Rushing[4], Isabelle Lemasson[4], Sydney Wilson[1], Dominic Sales[1], Edward W. Harhaj[5], Murali Janakiram[6], B. Hilda Ye[7], Zafar K. Khan[1], and Pooja Jain[1*]

[1]Department of Microbiology and Immunology, Drexel University College of Medicine, Philadelphia, PA, USA; [2]Instituto de Ciencias Biológicas, Universidad de Pernambuco, Recife, PE, Brazil; [3]Laboratory of Molecular Virology, George Mason University, Manassas, VA, USA; [4]Department of Microbiology and Immunology, Brody School of Medicine, East Carolina University, Greenville, NC, USA; [5]Department of Microbiology and Immunology, Penn State College of Medicine, Hershey, PA, USA; [6]Department of Oncology, Montefiore Medical Center,; [7]Department of Cell Biology, Albert Einstein College of Medicine, Bronx, NY, USA

Key words: HTLV-1, ATLL, Myocyte Enhancer Factor, MEF-2A, MEF-2C, Menin, Jun D

Running title: MEF-2 regulation of the 3'LTR of HTLV-1

*Address for correspondence: Pooja Jain, Ph.D.

Department of Microbiology and Immunology

Drexel University College of Medicine

2900 West Queen Lane, Philadelphia, PA 19129, USA

Phone: 215-991-8393; Fax: 215-489-4920, E-mail: pj27@drexel.edu

Abstract

Background. HTLV-1 is a complex human retrovirus and an etiologic agent causing a malignant and intractable T-cell neoplasia termed Adult T-cell leukemia and lymphoma (ATLL). Patients suffering from ATLL present with poor prognoses and a dearth of treatment options warranting a continuous need to develop novel therapeutic targets. In contrast to the HTLV-1 transactivator protein Tax, HTLV-1 bZIP protein (HBZ) maintains its expression in ATLL cells. The HBZ gene is encoded from the antisense strand of the provirus and is not under the transcriptional control of the 5' long terminal repeat (LTR) unlike other viral genes such as Tax. Few modifications have been reported in the 3'LTR, which regulates HBZ expression. Herein, we delineate the activities of a transcription factor MEF (Myocyte enhancer factor)-2 at both 5' and 3'LTRs in the context of ATLL progression and maintenance.

Results. In this study, we report that two MEF isoforms (2A and 2C) are highly overexpressed in acute ATLL patients from North America. These isoforms are recruited to the viral promoters at both the 5' and 3'LTRs. Their knockdown by shRNAs resulted in the downregulation of Tax and HBZ expression as well as a significant decrease in proliferation and cell cycle arrest in ATLL cells. Similarly, chemical inhibition of MEF proteins by MC1568 (a selective Class IIa HDAC inhibitor) resulted in the cytotoxicity of ATLL cells *in vitro* as well as reduction of proviral load and viral gene expression *in vivo*. At the molecular level, high enrichment of MEF-2C occurred at the 3'LTR along with cofactors Menin, Jun D, and Sp1/Sp3 thus providing a novel mechanism of regulation at the antisense promoter of HTLV-1.

Conclusions. This study establishes MEF-2 as critical players in ATLL, which interacts with Tax and HBZ at their respective promoters highlighting a novel mechanism of regulation at the 3'LTR involving Jun D and Menin. MEF signaling represent a potential target for therapeutic intervention.

Introduction

The development of adult T-cell leukemia/lymphoma (ATLL) is attributed to HTLV-1 infection (1-5), which infects an estimated 20 million people worldwide (6) with a recent outbreak among aboriginal populations in central Australia (7). HTLV-1 is endemic to regions of southwestern Japan, South American countries, equatorial Africa, and small groups in the Middle East (8-11). HTLV-1 possesses common retroviral genes including *gag*, *pol* and *env*, in addition to two regulatory genes, transactivation protein Tax and HTLV-1 bZIP factor (HBZ). Tax along with other viral genes are expressed through transcripts initiated by promoter activity from the 5'LTR region. The only protein encoded on the negative strand and transcribed from the 3'LTR is HBZ (12). ATLL cells from patients frequently express HBZ (13) while other viral proteins are transcriptionally repressed (14-16). HBZ inhibits Tax-mediated viral transcription from the 5'LTR via interactions with CREB/ATF that impede their DNA binding ability and thus prevent binding to Tax at the 5'LTR promoter. HBZ also interacts with cellular proteins of the AP-1 transcription factor family including c-Jun, JunB, and JunD, and modulates their transcriptional activity.

Previously, we showed that a member of the Myocyte enhancer factor 2 transcription family, MEF-2A, interacts directly with Tax at the 5'LTR and recruits transcriptional machinery such as CREB/p300 while disassociating the repressive histone deacetylase (HDAC) complex to promote viral gene expression and T-cell proliferation (17). MEF-2 is a member of the MCM-Agamous-Deficiens-Serum response factor (MADS) box group of transcription factors. The MEF-2 family consists of four isoforms (A-D, reviewed in (18)), which are well studied in the development of skeletal, cardiac, and neural tissues with established roles in embryogenesis. Interestingly, some of these isoforms play critical roles in T-cell development by regulating the transcription of the T-cell growth factor interleukin-2 (IL-2) (19). MEF-2 dysregulation has been

implicated in several T-cell leukemias/lymphomas including peripheral T-cell lymphoma (PTCL) (20) and T-cell acute lymphoblastic leukemia (T-ALL) (21).

In the study presented herein, we demonstrate the gene and protein level expression patterns of MEF-2 isoforms in multiple ATLL cell lines, and in a specific ATLL cohort termed North American (NA)-ATLL, which exhibit acute clinical manifestations with higher rates of aggressive subtypes compared to chronic counterparts (22). NA-ATLL patients demonstrate chemoresistance and a distinct pattern of somatic mutations (23). Most patients in this cohort showed drastically higher expression of MEF-2A; and also, of MEF-2C in a subset of patients. The transient silencing of both MEF-2A and MEF-2C decreased Tax and HBZ expression in ATLL cells. Similarly, chemical inhibition of MEF-2 by MC1568, a selective class I HDAC inhibitor known to suppress its activity (24-27), caused cytotoxicity exclusively in HTLV-1-infected T cells along with the downregulation of viral proteins in a MEF-2-dependent manner. Similarly, in HTLV-1-infected humanized mice, MC1568 exposure led to a reduction in the proviral load and viral gene expression. MEF-2 genes are required for G0/G1 transition in response to growth factor stimulation (28). Consequently, suppression of MEF-2A and MEF-2C expression led to a decrease in proliferation and cell cycle arrest of ATLL cells suggesting its involvement in ATLL pathogenesis. To further tease out the molecular mechanisms underlying MEF-2 activity in ATLL, we examined direct interactions of MEF-2A/C with HBZ and their recruitment to the 3'LTR along with Menin, a tumor suppressor protein. Together, these proteins assembled at the 3'LTR along with MEF-2A and MEF-2C provide a novel mechanism of transcriptional regulation of HBZ in the understudied antisense regulation of HTLV-1 gene expression. Collectively, these studies shed light on the complex mechanism of ATLL pathogenesis, HTLV-1 gene regulation from the 3'LTR and establishes MEF-2 signaling as a potential target for therapeutic intervention.

Results

MEF-2A and MEF-2C are the predominantly expressed isoforms in HTLV-1/ATLL cell lines. Due to the varying sensitivities of cell lines to culture conditions, and to ensure the utilization of exponential growth phase culture, we first sought to verify cell viability by assessing cellular metabolism with the Vybrant® MTT Cell Proliferation Assay. As shown in Figure S1A, all cell lines maintained at least 85% viability at peak growth except for SLB-1 and M8166 which exhibited slightly less viability. We next determined the number of integrated copies of HTLV-1 DNA per cell for each cell line through amplification of the HTLV-1 pX region by qPCR (Fig. S1B, C). Standard curve-based analysis revealed that SLB-1, ATL-2, ATL-ED and M8166 contained only 1-2 copies per cell of HTLV-1 provirus, in line with what is known for ATLL patients (29). As reported in the literature, MT-2 cells possessed 7 copies of integrated viral DNA per cell (29) similar to SP cells, while MT-4 had the highest copy number with approximately 25 per cell. Due to the varying number of HTLV-1 DNA copies among cell systems, we asked whether viral mRNA or protein expression levels would correlate with genome copy number. Western blot analysis showed comparable HBZ expression across all cell lines tested (Fig. S1D). Tax and p19 expression were mostly observed in viral-producing, non-ATLL-like cell lines such as MT-2, MT-4 and SLB-1 with the exception of ATL-2, which displayed both p19 and Tax expression at substantial levels. As expected, M8166 cell line exhibited high expression of Tax. Extracellular secretion of p19 was also reflected in MT-2, MT-4 and SLB-1 cells, confirming the viral-producing status of these cell lines (Fig. S1E, F). For some of the cell lines, FACS phenotyping was conducted to confirm their T-cell status and intracellular Tax presence (Fig. S1G). By combining these results, we categorized the studied cell systems into two groups: 1)

115 viral-producing cells such as MT-2, MT-4, and SLB-1; 2) non-viral-producing ATLL-like cells
116 such as ATL-2S, SP, ATL-55T, ATL-ED, and M8166.

117 To determine the expression of MEF-2 isoforms at the mRNA level, RT-qPCR was
118 performed on all cell lines as well as naïve and activated T cells ($CD3^+/CD28^+$), which were used
119 as references for gene expression and determination of fold-change, respectively. There was a
120 significant upregulation of MEF-2A mRNA in all cell lines, specifically in MT-4, SP, ATL-ED,
121 and M8166 cells which demonstrated up to 100,000-fold-change compared to Jurkat (Fig. 1A).
122 MEF-2B levels did not differ from Jurkat, except in M8166 cells but this difference was not
123 significant. However, MEF-2C showed significant upregulation in all cell lines (up to 100-fold
124 change), except in SP, ATL-55T, and M8166. However, MEF-2D expression levels remained
125 unchanged across all cell lines except for ATL-ED. Overall, these results suggest that MEF-2A is
126 highly overexpressed upon HTLV-1 infection and is maintained among non-viral producing ATLL
127 cell systems. The upregulation of MEF-2C mRNA suggests its involvement in the infection profile
128 but may be playing an ancillary role in ATLL pathogenesis along with MEF-2A, which needs
129 further investigation. Furthermore, we validated mRNA changes for MEF-2 isoforms at the single-
130 cell level within $CD4^+$ T-cell populations by a novel PrimeFlow™ RNA assay. As shown by the
131 flow cytometry histograms, MEF-2A expression peaks shifted among cell lines compared to Jurkat
132 (Fig. S2A). This was true of MEF-2C in the case of SLB-1, SP, ATL-2, and M8166, whereas MT-
133 4 and ATL-ED displayed a moderate increase. In addition, to HTLV-1/ATLL cell lines, some
134 HTLV-1-negative non-ATLL lymphoma cell lines were also analyzed for MEF-2 expression that
135 revealed a slight increase in MEF-2C mRNA expression, while other isoforms showed no change
136 (Fig. S2B). However, the observed fold change was significantly lower than that of ATLL cell
137 lines.

To determine whether MEF-2 isoform mRNA expression is reflected at the protein level, western blotting was performed with the same cell lines. Consistent with the mRNA expression, western blotting showed an increase in MEF-2A expression in almost all cell lines in comparison to Jurkat, naïve and activated T cells (Fig. 1B). Except for MEF-2B the remaining MEF-2 isoforms showed increased expression with activation of T cells ($CD3^+/CD28^+$). Although we saw an increase in expression of MEF-2C between naïve and activated T-cells, we also observed a post-translational modification (a distinct upper band) in most of infected cell lines, except for MT-4 and SP (Fig. 1B), which may suggest a divergence of activity in MEF-2C in these cell types. This modification, which may represent a phosphorylated or ubiquitinated form, may be speculated to dictate the activity of MEF-2C in various ATLL cell lines. Another important observation is the downregulation of MEF-2B in the majority of the ATLL cell lines (Fig. 1B), which has previously been shown to function as a tumor suppressor (30). The expression of MEF-2D showed increased levels in activated T cells but remained similar in all the ATLL cell lines (Fig. 1B). To quantitatively corroborate our western blotting results, we utilized automated capillary-based protein electrophoresis that provides quantitative values of protein expression (Fig. 1C). Comparable to the results from conventional western blotting, we observed a similar pattern of increased MEF-2A expression. Altogether, these results provide additional support for MEF-2A and MEF-2C in HTLV-1/ATLL pathogenesis.

***Knockdown of MEF-2A and MEF-2C downregulates HBZ* expression.** Since we observed increased expression of MEF-2A and MEF-2C in ATLL cell lines, we wanted to address the role of these two isoforms in ATLL by performing MEF-2A/C knockdown (KD) studies in ATL-ED, a representative Tax-negative cell line, and MT-4, a Tax-positive virus-producing cell line. We

transfected the cells with either siMEF-2A or scrambled siRNA (Fig. 2A). We analyzed MEF-2A expression along with other isoforms by RT-qPCR to determine potential compensatory effects following MEF-2A KD. We noticed that there was a dose-dependent downregulation of MEF-2A in both cell lines but did not observe any changes for the other isoforms. Interestingly, HBZ was significantly downregulated in both cell lines in a dose-dependent manner (Fig. 2A). When MEF-2A was depleted in MT-4 cells, a slight decrease in MEF-2C expression was observed at the highest concentration of siRNA. As expected, a significant dose-dependent reduction of Tax and HBZ was observed (Fig. 2A). To assess the effects of MEF-2C depletion, we performed siRNA-mediated MEF-2C KD in ATL-ED and MT-4 cells. MEF-2C expression decreased at both the mRNA (Fig. 2B) and protein (data not shown) levels in an siRNA dose-dependent manner. Likewise, mRNA expression of HBZ and Tax was assessed by RT-qPCR in MT-4 cells; however, a significant decrease in HBZ was only seen at the highest siRNA concentration (Fig. 2B). Following MEF-2C KD, Tax mRNA was only downregulated upon transfection of 50 nM of MEF-2C siRNA. These results indicate that MEF-2A and MEF-2C KD in ATL-ED and MT-4 significantly downregulate HBZ and are essential for its transcriptional activity.

Knockdown of MEF-2A and MEF-2C decreases proliferation and cell cycle progression in ATLL cell lines. We next sought to elucidate how MEF-2 isoforms modulate various physiological and phenotypic changes in ATLL cell lines. We assessed whether transiently silencing MEF-2A and MEF-2C could alter the phenotypic state of the ATLL cell lines utilized in this study. We transiently transfected MEF-2A and 2C siRNAs along with scrambled controls in Jurkat, ATL-ED and MT-4 cells. We subsequently observed depletion of both MEF-2A and MEF-2C at the 50 nM concentration (Fig. 3A). To assess the phenotypic state of these cell lines, we analyzed

proliferation status and cell cycle progression. We determined the proliferation profile of these cell lines via Ki-67 staining and flow cytometry following siMEF-2A/2C treatment as compared to scrambled siRNA. The presence of Ki-67 at specific phases of the cell cycle serves as a surrogate for proliferation. We stained all three representative cell lines, Jurkat, ATL-ED, and MT-4 with Ki-67 after transfection with either MEF-2A, MEF-2C or control siRNAs (Fig. 3B). We observed decreased Ki-67 expression in the siMEF-2 transfected samples compared to scrambled controls, suggesting that the proliferation of these ATLL cell lines was inhibited via MEF-2A/C knock down. However, we observed only a 3% decrease in proliferation in uninfected Jurkat cells after MEF2 KD, whereas ATL-ED exhibited 26% and 32% decrease in proliferation with siMEF-2A and siMEF-2C respectively (Fig. 3B). Similarly, in MT-4 cells there was a significant inhibition of proliferation, with a 43% decrease with siMEF-2A and 46% decrease with siMEF-2C, compared to scrambled control. Due to the dramatic effects of MEF-2 depletion on the proliferation of these ATLL cell lines, we next sought to determine if there were any perturbations in cell cycle regulation, which could explain such changes in phenotype. To this end we performed propidium iodide (PI) staining to label and quantify the different phases of the cell cycle. We carried out similar knockdown experiments with siMEF-2A and siMEF-2C and observed the various cell cycle phases with histogram plots. We observed significant alterations in the cell cycle profiles in representative ATLL cell lines compared to Jurkat cells. Moreover, we noticed a profound change in cell cycle progression of ATLL cells transfected with siMEF-2A and siMEF-2C compared to scrambled controls (Fig. 3C). In Jurkat cells, there was a modest decrease in the G2-M proliferating cells comparing scrambled control and siMEF-2, whereas in ATL-ED and MT-4 cells there was an accumulation of cells in the G1-S phase and a ~50% decrease in the G2-M mitotic cells when transfected with siMEF-2A or siMEF-2C. Similarly, cell cycle progression was suppressed in MT-

4 cells, which exhibited G1 accumulation of 64% with siMEF-2A and 58.6% with siMEF-2C respectively, compared to scrambled control (29.3%). There was also a significant decrease in mitotic cells from 57.8% (scrambled control) to 13.8% (siMEF-2A) and 13.7% (siMEF-2C), respectively (Fig. 3C). Thus, we inferred that these perturbations in the cell cycle resulted in decreased proliferation and likely loss of cell viability. The percentage of cells in the G2-M phase of the mock transfected Jurkat, ATL-ED and MT-4 consisted of nearly 50% of cells in the mitotic phase and active proliferation. After transfection with siMEF-2A or siMEF-2C, the percentage of cells in G0-G1 phase increased, suggesting that MEF-2A/C KD led to a suppression in cell cycle progression in actively proliferating ATLL cells, causing cell cycle arrest in the G1-S phase (Fig. 3C), potentially leading to apoptosis or another form of cell death.

Chemical inhibition and siRNA-mediated knockdown of MEF-2A/C modulates viral gene expression in vitro and in vivo: For knockdown studies we had chosen a specific dose and duration of siMEF-2A and siMEF-2C treatment that did not induce cell death, so as to ascertain physiological differences in the transcription of viral genes. However, to study the role of MEF-2 in ATLL cell line survival, we resorted to a specific Class IIa HDAC inhibitor (HDACi) termed MC1568, that could inhibit MEF-2 activity. Due to the known interactions between MEF-2, class IIa histone deacetylases (HDACs) (31, 32), and associated repressor complexes that keep MEF-2 isoform(s) expression in a repressed state (25, 33), we aimed to investigate the effect of MC1568 (24-27) on MEF-2 activity in ATLL cells. To examine cell viability following MC1568 treatment in HTLV-1-infected ATLL cell lines, we performed an MTT cell proliferation assay to derive IC_{50} curves. We calculated IC_{50} curves for primary activated T cells, Jurkat, ATL-ED, and MT-4 cells (Fig. 4A). There was no toxicity in activated T cells and calculated IC_{50} values of 3.011μM and

0.389μM for ATL-ED and MT-4, respectively. Furthermore, we derived an IC_{50} value of 13.38μM in Jurkat cells, supporting the ATLL-specific cytotoxic activity of MC1568.

To ensure that the observed cytotoxic activity was due to specific inhibition of MEF-2 activity, we established combinatorial treatments by first knocking down MEF-2A or MEF-2C via siRNA transfection and then derived MC1568 IC_{50} values for Jurkat, ATL-ED, and MT-4 cell lines. Here, we observed that MEF-2A knockdown resulted in increased IC_{50} values for MT-4 and ATL-ED cells, and Jurkat cells exhibited no cytotoxicity. In a similar experiment with siMEF-2C, MT-4 and ATL-ED showed no cytotoxicity compared to non-transfection conditions (Fig. 4B). Furthermore, we transiently silenced serum response factor (SRF) in these same cell lines as an additional control to determine whether the activity of MC1568 was specific to MEF-2 isoform(s). SRF is a transcription factor that is in the same family as MEF-2 and has similar interactions with class II HDACs (34, 35). We noticed that SRF knockdown resulted in no or modest change in IC_{50} values as shown in Fig. 4B compared to the original IC_{50} values derived from cells not transfected with siRNA in all three cell lines. To ascertain that observed effects are HTLV-1 mediated, we performed gain in function studies with pSG-Tax-His and pSG-HBZ-His overexpression plasmids in all three cell types. As expected, Jurkat did not show any real change in IC_{50} values but both ATL-ED and MT-4 cells showed increase in IC_{50} upon HBZ (3.02/11.7 um, 0.38/1.32 um, respectively) and Tax (3.02/16.65 um, 0.38/2.65 um, respectively).

To assess the *in vivo* effects of MC1568 treatment, humanized NOD/SCID/γ-null mice were injected with MT-2 cells for 2 weeks to establish HTLV-1 infection. Mice were then stratified into vehicle control groups and treatment groups. We assessed proviral load in the blood and spleen of MC1568-treated mice and observed a significant decrease with MC1568 treatment (Fig. S3). We isolated PBMCs from the blood of the control and the treated animals via Ficoll-paque based gradient isolation and isolated DNA using aforementioned methods; we also obtained RNA from the same process which was then converted into cDNA. Between the control and the treated

groups, there was a decrease of at least 10 copies of Tax and HBZ in the DNA, and a 10-to-20-fold decrease of Tax expression, but a massive downregulation of HBZ at the RNA level (Fig. S3A). Similarly, there was a significant downregulation of Tax and HBZ by at least 10 copies in the spleens of the control and treatment groups. Furthermore, we observed a 15 to 20-fold decrease in the expression of Tax and at least a 100-fold decrease of HBZ, respectively (Fig. S3B).

MEF-2A and MEF-2C are significantly upregulated in an acute NA-ATLL patient cohort. To ascertain the clinical importance of MEF-2 isoforms, we investigated their expression and relevance within patient cohorts. We obtained mRNA from PBMCs of North American ATLL (NA-ATLL) patient cohorts (23, 36), along with seronegative, asymptomatic carriers (ACs) and HAM/TSP patients from the same geographic areas of and South America. We performed RT-qPCR and derived the relative fold-change in comparison to activated PBMCs as a reference. Following our characterization of ATLL cell lines and MEF-2A/C knockdown, we anticipated higher expression of MEF-2A and/or MEF-2C in the NA-ATLL samples. Our results showed a significant logarithmic increase of MEF-2A in NA-ATLL samples ($p<0.05$) but did not show a noticeable fold-change in comparison to other stratified groups of seronegative, ACs and HAM/TSP patients (Fig. 5). Differences in MEF-2B and MEF-2D expression were not statistically significant. We noticed a logarithmic fold-change in MEF-2C expression in more than half of the NA-ATLL samples, but the other half of the samples displayed low to modest expression and did not achieve statistical significance. We also assessed three immortalized NA-ATLL patient-derived cell lines (ATL13, ATL18, ATL21) (23) for MEF-2 isoform and viral protein expression (Fig. S4A, B). The increased expression of Tax and HBZ correlated with increased expression of MEF-2A and 2C or vice-versa in ATL18 and ATL21 cell lines. Similarly, ATL13 cells, the

absence of MEF-2A/2C correlated with lower viral protein expression suggesting a linkage between MEF-2 isoform expression patterns and the expression of viral proteins. For further verification of these findings, we quantified protein lysates from ATL-18 and ATL-21 cells using capillary electrophoresis to obtain a quantitative readout and virtual plot generated using WES compass software (Fig. S4C), which yielded a similar pattern of expression in patient cell lines compared to Jurkat cells.

MEF-2A and MEF-2C are enriched in the 3'LTR and bind with HBZ to control viral expression via activation of MEF-2A/C. We previously reported that MEF-2A is enriched in the 5'LTR of the provirus and interacts with Tax to regulate viral gene expression (17), but it remains unclear how viral gene expression is controlled at the 3'LTR. To this end, we first examined localization of MEF-2 isoforms and HBZ in ATL-ED cells at the steady state by nuclear/cytoplasmic fractionation. We observed that only MEF-2A and MEF-2C were present in the nuclear fraction along with HBZ (Fig. 6A). We then evaluated enrichment of MEF-2 isoforms (A and C), viral proteins (HBZ and Tax), and various co-factors including Menin, Jun D, C/EBPα (known transcriptional repressor of HTLV-1 5'LTR (37)) as well as Sp1/Sp3 (known activator of 3'LTR (38)) at the both promoter sites. NR4A1 promoter was utilized as a control, which has been shown to be occupied by MEF-2 in T cells (39) thus serving as a canonical MEF-2 binding (Fig. 6A). ATL-ED being Tax negative did not show any recruitment of Tax on the 5'LTR (Fig. 6B) although considerable recruitment of RNA pol II, MEF-2A, and CREB was observed, which is a known binding factor at CRE elements at the 5'LTR (40). Interestingly, high level enrichment of CEBPα, but not Sp1/Sp3, was observed at this site. Presence of HBZ was also detected, which is known to bind with C/EBPα to inhibit the activation of HTLV-1 5'LTR (41). Together, these observations

explain blockade of transcription from 5'LTR in ATL-ED cells. At the 3'LTR, we observed a basal level enrichment of MEF-2A and a much higher recruitment of MEF-2C along with JunD, Menin, Sp1 and Sp3 but not C/EBPα representing a transcriptionally active state (Fig. 6C). Interestingly, at the NR4A1 promoter, both repressor and activator were recruited in exact same proportion (Fig. 6A) thus reaffirming our previous observations (37, 38) about the ratio of activators and repressors being the key for controlling transcription at a particular promoter site.

To further assess the mechanistic aspects of MEF-2 effects on HBZ, we overexpressed HBZ in Jurkat cells and performed co immunoprecipitation to assess the binding. MEF-2A interacted weakly but MEF-2C strongly with HBZ (Fig. 7A). A reciprocal binding assay was performed in ATL-ED cells with endogenous MEF-2A/2C to investigate the binding of HBZ and Menin, a tumor suppressor that is downregulated in ATLL (42). Both MEF-2A and MEF-2C interacted with Menin at steady state in ATL-ED, MT-2 and MT-4 along with HBZ but not in Jurkat, indicating that these proteins exist in the same complex (Fig. 7B). Additionally, we examined the binding of Menin and JunD in ATL-ED cell compared to Jurkat cells, and found that Menin did not bind to JunD in ATL-ED cells (Fig. 7C). To investigate this further, we transiently knocked down both MEF-2A/2C by siRNA and in the absence of MEF-2A/2C, there was no recruitment of JunD compared to scramble control that showed 20-fold enrichment of JunD at the 3' LTR (Fig. 7D), in the presence of both MEF-2A and MEF-2C isoforms. Together, these data demonstrate that MEF-2C forms complexes with HBZ and Menin at the 3'LTR, which liberates JunD to activate the antisense promoter.

Discussion

Extensive efforts have been underway to understand the etiology and pathogenesis of HTLV-1-induced leukemogenesis, although much remains unknown. Our previous study identified a role for MEF-2 in facilitating T-cell transformation and leukemogenesis via Tax-mediated LTR activation and viral replication (17). We observed increased MEF-2 expression in ATLL patients compared to controls, however, additional studies were required to elucidate the role of MEF-2 isoforms. Here, we present data that implicates the MEF-2A/C isoforms in exacerbating aggressive carcinogenesis and related symptoms in North American ATLL patients.

First, we characterized several active HTLV-1 producing and non-HTLV-1 producing ATLL-like cell lines by determining virion copy number and protein levels of Tax and HBZ. We observed consistent level of HBZ expression across all cell lines, whereas higher HTLV-1 DNA copy number and Tax expression were only observed in the viral-producing cell lines. These results support a recently proposed model of sporadic Tax expression and its potential function as an immunodominant epitope (43). We then examined MEF-2 isoform expression in HTLV-1 positive cell lines and ATLL cell lines to ascertain whether differential expression could be facilitating ATLL progression/development. The data presented in Fig. 1A clearly shows consistently upregulated MEF-2A and MEF-2C mRNAs in viral-producing cell lines compared to control Jurkat cells, although MEF-2A displays significantly higher expression compared to MEF-2C. These two isoforms also exhibit increased mRNA expression in most of the ATLL cell lines examined, indicating that variability in expression exists between ATLL patients. These expression patterns were further confirmed with single cell-based RNA priming in real-time, which yielded similar results of higher MEF-2A expression in ATLL cell lines. Interestingly, only MEF-2C mRNA was upregulated in non-ATLL cells compared to MEF-2A except in Ly13.2 cells

where both isoforms showed a modest increase, suggesting a potentially synergistic role for MEF-2C in leukemogenesis rather than a role in viral pathogenesis. This also suggests that higher expression of MEF-2A is specific to HTLV-1-induced ATLL cell lines as observed in Fig. 1. Furthermore, we corroborated protein expression levels using naïve and activated $CD3^+/CD28^+$ T cells as controls to differentiate activation versus infection-mediated changes in MEF-2 isoforms, which revealed that the overexpression of MEF-2A was more of a viral mediated effect rather than the activation of lymphocytes. However, the expression of MEF-2C was probably more of a T cell activation phenomenon together with post-translational modifications, which may or may not be viral mediated. This additional slower migrating band observed in western blots is absent in uninfected Jurkat and MT-4 cell lines; the latter of which has defective reverse transcriptase (40, 41), suggesting that this modification could be an activation phenomenon, although the precise mechanism remains to be determined. We also noticed that the expression of MEF-2B was diminished in activated T cells. Although MEF-2B mRNA levels for all cell lines were comparable to Jurkat there was a clear downregulation of MEF-2B at the protein level across all cell lines. Furthermore, we also observed similar MEF-2A expression patterns in a capillary-based electrophoresis approach, where there was increased expression of MEF-2A in all cell lines except SP cells, which is an IL-2-dependent cell line that contains only one copy of the virus in its genome (44). Similarly, M8166, a lymphoblastoid cell line that harbors a defective provirus of HTLV-1 did not demonstrate increased MEF-2A expression (45). Additionally, there was significantly increased expression of MEF-2C in MT-2, MT-4, SLB-1 and ATL-ED, but not as much in the other cell lines; this heterogeneity of expression of MEF-2C needs more investigation. These results suggest a potential positive correlation between increased MEF-2A expression and viral copy number. In line with the current literature, our results suggest a role for MEF-2B as a tumor

suppressor, where downregulation of MEF-2B promotes ATLL pathogenesis (30). Collectively, these results demonstrate that MEF-2A is the predominantly expressed isoform across most ATLL cell lines while MEF-2C was overexpressed in some of the ATLL cell lines and mostly in the non-ATLL cell lines.

Previous studies have conducted MEF-2 isoform-specific knockdown and knockout experiments to elucidate their distinct functions in various tissue types; however, our understanding of the roles of MEF-2 isoforms in ATLL is severely lacking. Here, we performed MEF-2A and MEF-2C knockdown studies in representative cell lines, ATL-ED ($HBZ^{+}Tax^{-}$) and MT-4 ($HBZ^{+}Tax^{+}$). Following knockdown of MEF-2A, there was a significant downregulation of HBZ in both cell lines, which suggests a direct correlation between MEF-2A and HBZ. We also observed downregulation of Tax in MT-4 cells following MEF-2A knockdown, which reaffirmed our earlier studies. Since there was increased MEF-2C expression in most ATLL cell lines, we transiently knocked down MEF-2C in ATL-ED and MT-4 cells and observed downregulated HBZ mRNA in ATL-ED, even at the lowest siRNA concentration. Although HBZ was downregulated in MT-4 cells, there was only a modest decrease in Tax expression at the highest siRNA concentration. These data suggest that MEF-2C is more important in the regulation of HBZ expression, but in the presence of Tax may play an ancillary role to MEF-2A, suggestive of a more synergistic relationship. We hypothesize that both MEF-2A and MEF-2C have overlapping functions in HTLV-1 pathogenesis in conjunction with both Tax and HBZ. It was evident from the proliferation and cell cycle profile analysis that both of the genes are necessary for the maintenance of highly proliferative mitotic cells in MT-4 and ATL-ED. Nonetheless, the negligible decrease in the proliferation of Jurkat cells may be due to its immortalization and presence of SV40 T antigen. Similarly, there was a difference in cell cycle progression compared to controls wherein we

observed a block in G1-S transition in si-MEF-2A/2C transfected cells thus impeding the transition of S-phase cells to highly proliferating mitotic cells. From the literature there is a requirement of MEF-2 isoform(s) in cell cycle progression, and unscheduled MEF-2 transcription during the cell cycle reduces cell proliferation, which may also occur after knockdown of MEF-2A and 2C in ATLL cell lines (46).

Due to the lack of standard of care for ATLL, we assessed the efficacy of pharmacological inhibition of MEF-2 using MC1568, a selective class IIa HDACi known to repress MEF-2 activity in muscle cells (25, 26). We treated representative ATLL cell lines with MC1568 alone and we observed no toxicity in activated T cells. However, there was significant cytotoxicity in ATL-ED and MT-4 cells, although the IC_{50} curves were in the micromolar range at 3.0 μM and 0.38 μM, respectively. Our results indicated that the cytotoxicity in ATLL cell lines was associated with the MEF-2 pathway and not any other MAPK pathway. However, we observed a high IC_{50} value in Jurkat cells (13.38 uM) compared to the ATLL cell lines, therefore cytotoxicity increases due to the presence of HTLV-1. In order to determine whether the cytotoxicity was associated with MEF-2 suppression, we performed combinatorial experiments by transiently knocking down MEF-2A or MEF-2C and treating with MC1568. When either MEF-2A or MEF-2C were transiently silenced followed by MC1568 treatment, MEF-2A knockdown resulted in a nearly 20-25-fold increase in IC_{50} values, 20.96 uM and 25.68 uM, in MT-4 and ATL-ED, respectively. Similarly, when MEF-2C was transiently silenced in combination with MC1568, there was no cytotoxicity in both ATLL cell lines. We also knocked down SRF, which is involved in the same signaling pathway as MEF-2 (34, 35), and observed little to no change in IC_{50} values with similar values compared to siRNA negative treatments. Together, these experiments argue for specificity of targeting of the MEF-2 signaling pathway and no other signaling molecules. Additionally,

overexpression of Tax, in ATL-ED cell increased the IC_{50} values 4-fold, suggesting that the drug has effects on viral genes, since the IC_{50} values did not change in Jurkat cells. The overexpression of Tax is likely promoting the proliferation (47, 48) of the cells and possibly contributing an adjunct role to the pathogenesis of HBZ in ATL-ED cells thus resulting in an increase in the IC_{50} in ATLL cells but not in Jurkat.

Moreover, in the NOD/SCID ATLL humanized mouse model we observed a significant decrease in viral gene copy numbers when treated with MC1568 as well as decreased expression of Tax and HBZ at the mRNA level thus substantiating the effect of MC1568 in regulating the activity of MEF-2 complexes *in vivo* both in the blood and spleen. *In vivo* activity of MC1568 exhibits less toxicity in mice at a dosage of 50 mg/kg and has been shown to decrease the proliferation of epithelial testicular carcinoma cell lines (24). Our results provide proof of concept that chemical inhibition of MEF-2 can downregulate HTLV-1 gene expression *in vivo* and is translatable in an animal model of ATLL.

Since there was elevated MEF-2A and MEF-2C expression in viral-producing and ATLL cell lines, we wanted to assess MEF-2 isoform expression patterns in patient samples to ensure clinical relevance. We characterized a specific HTLV-1-infected NA-ATLL patient cohort (22, 23, 36) for expression of MEF-2 isoforms and observed a significant logarithmic increase in the expression of MEF-2A in ATLL patients compared to seronegative, asymptomatic carriers and also HAM/TSP patients. We observed a similar trend with MEF-2C expression in a subset of ATLL patients, although they were not statistically significant. Nonetheless, there was divergent MEF-2B and MEF-2D expression in NA-ATLL patients, where certain subsets of patients exhibited increased MEF-2B/D expression while others exhibited little to no expression. This range of expression across patient samples resulted in differences not deemed significant within

each patient group. The correlation between viral proteins and MEF2A/C strongly suggest that there is evidence of synergy of Tax and MEF-2A and MEF-2C in patient cell lines. In the ATL-18 and ATL-21 cell lines, the expression of MEF-2A and MEF-2C correlated with the presence of Tax and HBZ expression.

Our previously published data demonstrated that MEF-2A was recruited to the 5' viral LTR for transactivation by Tax (17). Our current results indicate that at steady state MEF-2A and MEF-2C are present in the nuclear fraction and not in the cytoplasmic fraction suggesting they might be continuously transcribing viral genes. The recruitment of both MEF-2A and MEF-2C to the 3'LTR of the virus in ATL-ED cells, which lacks Tax transactivation at the 5'LTR as shown in Fig. 6B confirms that they are present at the anti-sense region of the viral LTR. We also precipitated various known targets that are enriched in the 3'LTR of the virus along with MEF-2A and MEF-2C to examine how the transcriptional profiles are enriched in the viral LTRs. Although MEF-2A and MEF-2C were recruited to the 5'LTR along with HBZ, Menin and members of the Sp family, there was also a significant upregulation of CEBP-α (CCAAT/enhancer-binding proteins) which serves as an inhibitory factor of transcription at the 5'LTR, thus potentially explaining why the 5'LTR is transcriptionally silent (37). At the 3'LTR there was a significant increase in the Sp-1 family of transcription factors along with enrichment of JunD and Menin (49, 50). Interestingly, there was a significantly higher enrichment of MEF-2C compared to MEF-2A at the 3'LTR, suggesting that MEF-2C may be playing a more important role in the transcriptional activity at the 3'LTR. Based on the enrichment of MEF-2A and MEF-2C at the 3'LTR, we were interested in the protein-protein interactions that occurred between MEF-2 and HBZ, along with JunD and Menin. Protein binding assays revealed that HBZ could interact with both MEF-2C and MEF-2A in Jurkat cells, but MEF-2A binding was rather modest. However, when we performed a reciprocal

immunoprecipitation with endogenous proteins in ATL-ED cells, MEF-2A and MEF-2C interacted with both HBZ and Menin in three different representative ATLL cell lines, including ATL-ED. Furthermore, we observed that Menin bound JunD in uninfected Jurkat cells but not in ATL-ED implying that different JunD complexes exist in ATLL cells. Taken together, MEF-2C binds Jun D and Menin, which is a tumor suppressor (51, 52) to regulate its transcriptional activity. Based on our data, we hypothesize that Menin interacts with MEF-2C and is sequestered along with HBZ, to prevent Menin binding with JunD, which subsequently allows JunD to mediate transcriptional activity along with HBZ at the 3'LTR. To this end, when MEF-2A and MEF-2C were transiently knocked down, we noticed that there was no enrichment of JunD at the viral LTRs, but we saw significant enrichment of JunD at the 3'LTR in the scrambled control. This observation implies that in the presence of MEF-2C or MEF-2A, Menin binds to MEF-2C and HBZ in a complex as seen in Fig. 7B&D and thus allows JunD to be recruited to the 3'LTR to activate transcription. However, in the absence of MEF-2A/2C the enrichment/recruitment of JunD to the 3'LTR is minimal suggesting there might be binding of Menin with JunD that could decrease its activity or enrichment. Mechanistically, the presence of MEF-2C at the 3'LTR is essential for the transcriptional activation of JunD and the antisense promoter of HTLV-1.

Taken together we posit that MEF-2A and MEF-2C may represent potential mechanistic targets in the pathogenesis of ATLL. Since MEF-2A and MEF-2C appear to be enriched in the 3'LTR of the virus, and the MEF-2A and HBZ interactions suggest this may be important for the antisense transcription of the viral genome. We speculate that MEF-2A and MEF-2C bind to HBZ in different chronological order to control the 3'LTR and viral pathogenesis. It is possible that a distinct transcriptional machinery may control the HTLV-1 3'LTR compared to the 5'LTR. Factors such as Menin, Sp-1 and AP-1 have already been studied in this regard (53-55). Therefore,

there is a possibility that these transcription factors may associate with MEF-2 to regulate the transcriptional activity at the 3'LTR. We have also demonstrated that MEF-2A and MEF-2C are essential at the 3' viral promoter for sequestering Menin and increasing JunD transcriptional activity. Finally, we have demonstrated a potential use of MC1568 for targeted treatment of ATLL by regulating MEF-2 isoforms as a target for HTLV-1-induced ATLL pathogenesis.

Conclusions

This study provides evidence for the involvement of MEF-2A and MEF-2C in the 3'LTR mediated anti-sense transcriptional program. The clinical relevance of this study is established via the overexpression of MEF-2A and MEF-2C in acute ATLL patients and patient-derived cell lines and showcases how MEF-2 isoforms can modulate the proliferation and cell cycle regulation in ATLL cells. Moreover, in the absence of 5'LTR activity, MEF-2 can bind to relevant factors such as Menin and modify the activity of JunD and promote transcription from the 3'LTR of the virus.

Materials and Methods

Patient samples and primary cells. Samples from NA-ATLL patients, as published (22, 23, 56), were obtained from the Albert Einstein College of Medicine (NY, USA). In addition, samples from 11 HTLV-1-associated myelopathy/Tropical spastic paraparesis (HAM/TSP) patients (82% female) and 10 asymptomatic HTLV-1-infected individuals (60% female) were studied. These were followed up at a reference outpatient clinic of Infectious and Parasitic Diseases Service (DIP) at the Hospital Universitário Oswaldo Cruz (HUOC/UPE), located in Recife, Pernambuco, Brazil. HAM/TSP was diagnosed according to WHO guidelines. Samples from 10 non-infected healthy Brazilian individuals (70% female) were also included in this study. HTLV-1 serological screening

and confirmation (WB) was performed at HEMOPE Blood Bank Center, in Recife, Brazil. Infection was additionally confirmed at Fiocruz-PE Institute, also in Recife, Brazil, through qPCR using a previously described protocol (57). Samples were blinded throughout the study and categorized as control/seronegative, asymptomatic carriers (ACs), ATLL, and HAM/TSP. The median age range for females and males was: 46-49 and 38-45 (Control); 42-43 and 37.5-60 (ACs); 48-49 and 38-53 (ATLL); 45-48 and 46-59 (HAM/ TSP), respectively. PBMCs were isolated from Buffy Coat using Ficoll-Paque and T cells were isolated using a negative selection kit (Stem Cell Technologies, Vancouver, Canada). Activation of PBMCs was achieved by phytohemagglutinin (PHA) stimulation (2 mg/mL) for 3 days, as previously described (17). T cells were activated using ImmunoCult™ Human CD3/CD28 T Cell Activator kit (StemCell Technologies) for 2 days.

Cell lines. HTLV-1-transformed cell lines MT-2, MT-4 (58, 59), M8166 (60) and SP (HTLV-1-infected clone from PBMCs of an ATLL patient) (61) were obtained through the NIH AIDS Reagent Program (Catalog No. 237, 120, 11395 and 3059, respectively). HTLV-1-negative Jurkat cell line (E6-1, Cat No. 177) was also obtained from NIH while SLB-1 (62-65) and ATLL-derived cell lines, ATL-2(S) (14, 66, 67), ED-40515(-) (referred here as ATL-ED) (66-68), and ATL-55T were described previously (68, 69). Cultures were maintained in RPMI 1640 medium supplemented with L-glutamine (Atlanta Biologicals, Flowery Branch, GA), 10% fetal bovine serum (FBS, Atlanta Biologicals) and 1x Penicillin/Streptomycin (Gibco, Gaithersburg, MD) in a humidified incubator with 10% CO_2 at 37°C. SP culture was supplemented with 100 U/mL of human IL-2 (Peprotech Inc., Rocky Hill, NJ).

In addition, three NA-ATLL patient-derived $CD4^+$ T-cell lines (ATL13, ATL18, ATL21) were obtained from the Albert Einstein College of Medicine (NY, USA) and maintained in IMDM

with 100 units/mL IL-2 and 20% human serum. Two additional HTLV-1-negative human T-cell lines HUT78 and OCI-Ly13.2 were cultured in RPMI with 10% FBS while the third HH line was maintained in IMDM plus 20% FBS.

MTT cell viability/cytotoxicity assay. Before experiments, viability of all cell lines was assessed, and exponential phase cultures were utilized. Cells were seeded into 96-well plates at a density of 100,000 cells per well in Gibco's phenol red-free RPMI medium for 48 hours at 37°C in a humidified chamber. Cell viability was assessed using Vybrant® MTT Cell Proliferation Assay according to the manufacturer's protocol (ThermoFisher, Waltham, MA). Following the initial 48 hr incubation, 10 μL of 12 mM MTT was added to each well, then incubated for 4 hrs at 37°C before cells were lysed in 100μL of SDS-HCl solution. Cells were incubated for another 4 hrs at 37°C before final absorbance was measured at 570 nm (Sunrise™, Tecan, NC) as a direct assessment of viable cells in each culture. Similar MTT assays were utilized to test cytotoxic effects of MC1568 in a standard 2-fold dilution method with IC_{50} calculation by Prism8 software (GraphPad).

qPCR assay for determining integrated HTLV-1 copy number. Genomic DNA (gDNA) for each cell line was obtained using Qiagen's DNeasy Kit (Germantown, MD). Integrated HTLV-1 copy number was determined by performing quantitative polymerase chain reaction (qPCR) using the SYBR green assay (QuantStudio 6 Flex, Applied Biosystems, Foster City, CA) with GAPDH as an internal control and gDNA from the HTLV-1-infected rat cell line (TARL-2) as a reference since it carries one copy of provirus per cell (70). The following primer set was used to amplify the HTLV-1 regulatory Px region: 5'-CAAAGTTAACC ATGCTTATTATCAGC-3' (forward)

553 and 5'-ACACGTAGACTGGGTATCCGAA-3' (reverse). A standard curve for the Px region,
554 representing integrated HTLV-1, was generated from assay results using two-fold serial dilutions
555 of TARL-2 gDNA. The HTLV-1 copy number for each cell line was calculated from the standard
556 curve, using the respective CT values, and divided by the estimated number of cells (1ng DNA =
557 151.51 diploid cells).
558
559 **Western blotting for viral protein expression.** Protein lysates were extracted from transfected
560 cultures using Pierce RIPA Buffer supplemented with protease inhibitor cocktail
561 (Thermofisher Scientific) and phosphatase inhibitor Cocktail 3 (Sigma-Aldrich). Total protein
562 concentration was measured using a BCA protein assay and 25-30 μg of proteins were loaded per
563 lane in 4-15% gradient SDS-PAGE gels (Bio-Rad). Proteins were transferred onto PVDF
564 membranes at 4°C for 16-18 hours at 30V. Membranes were then blocked for 1 hour in 5% fat-
565 free milk in 1xTBS plus Tween 20. Images were read using the Gel Doc XR+ Gel Documentation
566 System (Bio-Rad) and processed on Image Lab software. Primary antibodies used were anti-HBZ
567 (dilution 1:1000; provided by Dr. Patrick Green), anti-Tax LT-4 (1:2000, provided by Dr. Yuetsu
568 Tanaka), and anti-p19 (1:1000; Zeptometrix, Buffalo, NY).
569
570 **Measurement of HTLV-1 infectivity (p19) via ELISA.** Supernatants from each cell line were
571 collected at 48 hrs in order to quantify extracellular levels of p19 protein released by each cell line.
572 Enzyme-linked immunosorbent assay (ELISA) was performed in duplicate for each cell line using
573 the HTLV p19 Antigen ELISA kit (Zeptometrix), according to manufacturer's instructions. The
574 final absorbance was measured at 450 nm (Sunrise™) and data was analyzed using the standard
575 curve method, which was generated from serial dilutions of the standards.

Phenotyping of cell lines by FACS. Jurkat cells and three virus-producing cell lines, MT-2, MT-4 and SP, were counted and 1 x 10^6 cells were surface stained for CD3 and CD4 using fluorochrome-conjugated antibodies, AF700 and FITC, respectively. Samples were incubated for 30 mins at 4°C in the dark. For intracellular staining of Tax, cells were fixed and permeabilized with 200 μL of permeabilization buffer followed by staining using 20 μL of PE-conjugated Tax antibody for 30 mins at 4°C in the dark. After incubation, cells were washed twice with 1x permeabilization buffer and resuspended with staining buffer for analysis by flow cytometry using BD FACS Calibur (BD Biosciences, San Jose, CA).

Analysis of MEF-2 isoform mRNA levels by PrimeFlow™ and RT-qPCR. The PrimeFlow™ RNA assay (Affymetrix, Santa Clara, CA) is an *in situ* hybridization assay that can detect target RNA transcripts at the single-cell level. mRNA levels of MEF-2 isoforms were assessed in the indicated HTLV-1-infected and uninfected cell lines using the PrimeFlow™ RNA assay according to the manufacturer's protocol. Cells were surface stained for anti-CD4 (PerCP Cy5.5) and individually hybridized with either an RPL13A probe (Alexa Fluor 488) to gate for transcriptionally active cells, or one of the four MEF-2 isoform probes (Alexa Flour 647 conjugated). Following target hybridization, signal amplification is accomplished through serial and sequential hybridizations of the highly specific PreAmplifier molecules, which only hybridize when both sides of the target probe pair are bound to the target RNA. Upon completion of the assay, the cells were analyzed using BD FACS Calibur (BD Biosciences). MEF-2 mRNA levels were also evaluated by RT-qPCR to validate PrimeFlow™ results. As previously described, RNA was converted into cDNA, which was then used as a template for qPCR amplification with primers given in (Supplemental Table 1). The fold-change expression was normalized to Jurkat and

599 calculated by $2^{-\Delta\Delta CT}$ method. Total RNA from patient samples was converted to cDNA and
600 amplified using standard real-time PCR. MEF-2 isoform fold-change expression was normalized
601 to activated PBMCs.
602
603 **MEF-2 isoform protein detection by western blot and WES (Protein Simple).** Western
604 blotting was performed as described above utilizing MEF-2 isoform (A-D)-specific antibodies
605 from Proteintech in the dilution of 1:1000. Automated quantitative protein analysis was performed
606 by WES (ProteinSimple, San Jose, CA) according to manufacturer's instructions. Lysates were
607 diluted to optimum concentration using Simple Western sample dilution buffer (ProteinSimple)
608 mixed with the fluorescent master mix and denatured at 95°C for 3 mins. Samples, primary
609 antibodies, and HRP-conjugated secondary antibodies were loaded in pre-assigned wells of a 25-
610 sample cartridge, then placed in WES instrument (Protein Simple). Primary antibodies were
611 titrated for WES and utilized in the dilution of 1:50 for MEF-2A, MEF-2B, MEF-2C, MEF-2D,
612 and Vinculin (R&D Systems, Minneapolis, MN). After capillary-based separation of the protein
613 samples and incubation with the primary and secondary antibodies, proteins were detected using
614 chemiluminescence. Protein signal and quantitation was generated automatically after each run
615 through the Compass for SW software. Detected protein quantities are presented as area under the
616 curve, normalized to vinculin as a loading control.
617 To assess MEF-2 isoforms in the nuclear-cytoplasmic fractions, cells were collected,
618 washed with PBS and then nuclear-cytoplasmic extracts collected using NucBuster™ Protein
619 Extraction Kit (MilliporeSigma, Burlington, MA). After isolation of the cytoplasmic fraction, the
620 cell pellet was sonicated along with reagent B and then supernatant was collected. Both the

cytoplasmic and nuclear fractions were probed for MEF-2A, -2B, -2C, and -2D (Proteintech) along with GAPDH as the loading control by western blotting.

siRNA transfection. Cells (3 x 10^5/well) were plated on 6-well plates and transfections were performed using Lipofectamine™ RNAiMAX (Invitrogen) according to manufacturer's protocol. Briefly, Lipofectamine™ and siRNA were diluted in Opti-MEM medium (Gibco). The diluted Lipofectamine™ and siRNA were incubated in a 1:1 ratio for 15 mins at room temperature. The siRNA-lipid complex was added to the corresponding wells. After 36 hrs. of incubation at 37°C, cell pellets were collected and processed to obtain total RNA (Qiagen RNAeasy mini kit) and protein, for RT-qPCR and western blotting, respectively.

Ki-67 and Propidium iodide staining. The representative cell lines were plated and subjected to siMEF-2A or siMEF-2C treatment at 25 nm concentration using Lipofectamine™ RNAiMAX (Invitrogen), along with negative scramble controls. The cells were collected 36 hrs post-transfection, washed with 1X PBS and cell pellets fixed with 2 mL of 70% ethanol overnight at -20°C. The cell suspension was resuspended with 20 μL of PE-KI-67 (BD Biosciences), mixed gently and incubated at room temperature for 30 mins. The cells were washed with 2 mL of staining buffer at 200xg for 5 mins and 500 μL of staining buffer was added to each tube and FACS analysis was performed. All cell lines were fixed in 70% ethanol at -20°C overnight after siRNA treatment as mentioned above. Cells were washed and RNase inhibitor and PI ready-probe reagent (Invitrogen) was added. The resulting DNA distributions were obtained by BD FACS Calibur (BD) and quantified for the proportion of cells in cell cycle phases using Flow-Jo software.

644 **In vivo testing of MC1568 in NOD/SCID/γ-null humanized mice.** Five-week-old female
645 NOD/SCID/γ-null (NODC57/BL) mice were housed and treated in accordance with Drexel
646 University laboratory animal resources guidelines and experimental protocols were approved by
647 the Institutional Laboratory Animal Care and Use Committee (IACUC). Each group had a total of
648 5 mice. Animals were irradiated within the first week of birth, receiving 10 million human $CD34^+$
649 cells, and then housed for 8-10 weeks. Once animals were 30% humanized, they received one
650 interperitoneally injected dose of 10 million irradiated MT-2 cells. The animals were housed for
651 another 2 weeks to allow for viral spread then stratified into vehicle control and treatment groups.
652 After the 2-week incubation, animals were treated with MC1568 (5mg/kg) at Day 0 and Day 3.
653 Animals were sacrificed 7 days post-MC1568 treatment. Spleens, liver, lung, brain, and blood
654 were collected post-mortem. The splenocytes and PBMC were isolated from spleens and blood,
655 respectively. RNA was then isolated using Trizol extraction protocol and converted into cDNAs
656 that were subjected to RT-qPCR to analyze expression of HBZ and Px region.
657
658 **Chromatin immunoprecipitation (ChIP) assay.** ChIP assays were performed using Pierce
659 Magnetic ChIP Kit (Thermo Scientific) per manufacturer's instructions with modifications for
660 non-adherent cells. Crosslinking and cell pellet isolation were performed using approximately
661 $4x10^6$ cells per ChIP. Briefly, cells were pelleted and fixed with 16% formaldehyde in serum free
662 media, quenched with 1x glycine and washed twice with 1x PBS. Steps for Lysis and MNase
663 digestion, IP elution, and DNA recovery was performed per manufacturer's protocol.
664 Immunoprecipitation was adjusted and combined such that magnetic beads, target antibodies
665 (Supplemental Table 2) and chromatin samples were incubated overnight at 4°C. DNA was then

eluted and subjected to RT-PCR using primers listed in supplemental Table 3. Samples were normalized to IgG for fold enrichment or adjusted based on 10% input for analysis.

Co-immunoprecipitation assays. For Co-IP, cells (Jurkat, ATL-ED, MT-2 or MT-4, as indicated) were lysed by sonication and cells lysates were pre-cleared with protein L magnetic beads. Samples were incubated overnight with 2mg of indicated antibodies and were washed to remove beads. Immunoprecipitated samples were resolved by SDS-PAGE and transferred to a PVDF membrane. Membranes were immunoblotted for either HBZ antibody or Menin and probed for the indicated markers. Where indicated, HBZ was over-expressed using a S-tag-HBZ plasmid in Jurkat cells and was pull down to detect its binding with MEF-2A and MEF-2C.

Declarations

Abbreviations

MEF-2 - Myocyte enhance factor-2

HTLV-1 - Human T-cell leukemia virus type 1

ATLL - Adult T-cell leukemia and lymphoma

C/EBP - CCAAT/enhancer-binding proteins

LTR – Long terminal repeat

HBZ – HTLV-1 bzip protein

Co-IP – Co immunoprecipitation

PCR – Polymerase chain reaction

Ethics statement

This manuscript utilizes patient-derived samples and data from the Albert Einstein College New York on a blinded basis. The patient cohort has been published before and was handled upon the institutional ethics committee approval.

Availability of data and materials

The datasets used and/or analyzed during the current study are available from the corresponding author on reasonable request.

Disclosure of Potential Conflicts of Interest

The authors declare there is no potential conflict of interest.

Authors' contributions

KM performed a majority of experimentation, conducted data analysis, and compiled the manuscript under direct guidance and supervision of PJ. JJ assisted in the completion of CHIP data, editing of the manuscript, and model creation. VT provided some patient data and associated text. ZKK and RG reviewed manuscript drafts and proofread final document before submission. CD extracted samples for mouse experiments under supervision from FK. DS performed experimentation with WES technique and contributed some data. SW extended some help in early drafts of manuscript. AWR provided preliminary CHIP data under the supervision of IL along with improvements to manuscript. MJ and EWH contributed to manuscript editing and improvements. BHY provided expert opinion and NA-ATLL samples. EWH and IL provided cell lines and plasmids used in the study and edited the paper. PJ conceptualized the study, provided intellectual insights to data analysis, finalized data flow and presentation for the submission of manuscript.

Consent to publish

All authors are in agreement to publish the content of this study as formulated.

Funding

These studies are fully supported by the funding from NIH/NINDS via R01 NS097147 to P.J.

Acknowledgements

We thank NIH AIDS reagents program for providing HTLV-1-infected/ATLL cell lines. HBZ antibody was a gift from Dr. Amanda Panfil, Ohio State University). TAX (LT-4) antibody was gifted by Dr. Yuetsu Tanaka (Japan).

References

1. Saito M, Jain P, Tsukasaki K, Bangham CR. HTLV-1 Infection and Its Associated Diseases. Leuk Res Treatment. 2012;2012:123637.
2. Nakao K, Abematsu N, Sakamoto T. Systemic diseases in patients with HTLV-1-associated uveitis. Br J Ophthalmol. 2018;102(3):373-6.
3. Eusebio-Ponce E, Anguita E, Paulino-Ramirez R, Candel FJ. HTLV-1 infection: An emerging risk. Pathogenesis, epidemiology, diagnosis and associated diseases. Rev Esp Quimioter. 2019;32(6):485-96.
4. Barrionuevo-Cornejo C, Duenas-Hancco D. Neoplastic hematological diseases associated with HTLV-1 infection. Semin Diagn Pathol. 2020;37(2):98-103.
5. Baratella M, Forlani G, Accolla RS. HTLV-1 HBZ Viral Protein: A Key Player in HTLV-1 Mediated Diseases. Front Microbiol. 2017;8:2615.
6. Coffin JM. The discovery of HTLV-1, the first pathogenic human retrovirus. Proc Natl Acad Sci U S A. 2015;112(51):15525-9.
7. Gruber K. Australia tackles HTLV-1. Lancet Infect Dis. 2018;18(10):1073-4.
8. Ngoma AM, Omokoko MD, Mutombo PB, Nollet KE, Ohto H. Seroprevalence of human T-lymphotropic virus (HTLV) in blood donors in sub-Saharan Africa: a systematic review and meta-analysis. Vox Sang. 2019;114(5):413-25.
9. Tabor E, Gerety RJ, Cairns J, Bayley AC. Did HIV and HTLV originate in Africa? JAMA. 1990;264(6):691-2.
10. Chihara D, Ito H, Katanoda K, Shibata A, Matsuda T, Tajima K, et al. Increase in incidence of adult T-cell leukemia/lymphoma in non-endemic areas of Japan and the United States. Cancer Sci. 2012;103(10):1857-60.
11. Gessain A, Mahieux R. Tropical spastic paraparesis and HTLV-1 associated myelopathy: clinical, epidemiological, virological and therapeutic aspects. Rev Neurol (Paris). 2012;168(3):257-69.
12. Gaudray G, Gachon F, Basbous J, Biard-Piechaczyk M, Devaux C, Mesnard JM. The complementary strand of the human T-cell leukemia virus type 1 RNA genome encodes a bZIP transcription factor that down-regulates viral transcription. J Virol. 2002;76(24):12813-22.
13. Polakowski N, Pearce M, Kuguyo O, Boateng G, Hoang K, Lemasson I. The splice 1 variant of HTLV-1 bZIP factor stabilizes c-Jun. Virology. 2020;549:51-8.
14. Taniguchi Y, Nosaka K, Yasunaga J, Maeda M, Mueller N, Okayama A, et al. Silencing of human T-cell leukemia virus type I gene transcription by epigenetic mechanisms. Retrovirology. 2005;2:64.
15. Tamiya S, Matsuoka M, Etoh K, Watanabe T, Kamihira S, Yamaguchi K, et al. Two types of defective human T-lymphotropic virus type I provirus in adult T-cell leukemia. Blood. 1996;88(8):3065-73.
16. Koiwa T, Hamano-Usami A, Ishida T, Okayama A, Yamaguchi K, Kamihira S, et al. 5'-long terminal repeat-selective CpG methylation of latent human T-cell leukemia virus type 1 provirus in vitro and in vivo. J Virol. 2002;76(18):9389-97.
17. Jain P, Lavorgna A, Sehgal M, Gao L, Ginwala R, Sagar D, et al. Myocyte enhancer factor (MEF)-2 plays essential roles in T-cell transformation associated with HTLV-1 infection by stabilizing complex between Tax and CREB. Retrovirology. 2015;12:23.
18. Madugula K, Mulherkar R, Khan ZK, Chigbu DI, Patel D, Harhaj EW, et al. MEF-2 isoforms' (A-D) roles in development and tumorigenesis. Oncotarget. 2019;10(28):2755-87.

19. Pan F, Ye Z, Cheng L, Liu JO. Myocyte enhancer factor 2 mediates calcium-dependent transcription of the interleukin-2 gene in T lymphocytes: a calcium signaling module that is distinct from but collaborates with the nuclear factor of activated T cells (NFAT). J Biol Chem. 2004;279(15):14477-80.
20. Tsukasaki K, Tobinai K. Human T-cell lymphotropic virus type I-associated adult T-cell leukemia-lymphoma: new directions in clinical research. Clin Cancer Res. 2014;20(20):5217-25.
21. Zuurbier L, Gutierrez A, Mullighan CG, Cante-Barrett K, Gevaert AO, de Rooi J, et al. Immature MEF2C-dysregulated T-cell leukemia patients have an early T-cell precursor acute lymphoblastic leukemia gene signature and typically have non-rearranged T-cell receptors. Haematologica. 2014;99(1):94-102.
22. Shah UA, Chung EY, Giricz O, Pradhan K, Kataoka K, Gordon-Mitchell S, et al. North American ATLL has a distinct mutational and transcriptional profile and responds to epigenetic therapies. Blood. 2018;132(14):1507-18.
23. Chung EY, Mai Y, Shah UA, Wei Y, Ishida E, Kataoka K, et al. PAK Kinase Inhibition Has Therapeutic Activity in Novel Preclinical Models of Adult T-Cell Leukemia/Lymphoma. Clin Cancer Res. 2019;25(12):3589-601.
24. Nebbioso A, Dell'Aversana C, Bugge A, Sarno R, Valente S, Rotili D, et al. HDACs class II-selective inhibition alters nuclear receptor-dependent differentiation. J Mol Endocrinol. 2010;45(4):219-28.
25. Nebbioso A, Manzo F, Miceli M, Conte M, Manente L, Baldi A, et al. Selective class II HDAC inhibitors impair myogenesis by modulating the stability and activity of HDAC-MEF2 complexes. EMBO Rep. 2009;10(7):776-82.
26. Panella S, Marcocci ME, Celestino I, Valente S, Zwergel C, Li Puma DD, et al. MC1568 inhibits HDAC6/8 activity and influenza A virus replication in lung epithelial cells: role of Hsp90 acetylation. Future Med Chem. 2016;8(17):2017-31.
27. Venza I, Visalli M, Oteri R, Cucinotta M, Teti D, Venza M. Class II-specific histone deacetylase inhibitors MC1568 and MC1575 suppress IL-8 expression in human melanoma cells. Pigment Cell Melanoma Res. 2013;26(2):193-204.
28. Di Giorgio E, Gagliostro E, Clocchiatti A, Brancolini C. The control operated by the cell cycle machinery on MEF2 stability contributes to the downregulation of CDKN1A and entry into S phase. Mol Cell Biol. 2015;35(9):1633-47.
29. Saito M, Matsuzaki T, Satou Y, Yasunaga J, Saito K, Arimura K, et al. In vivo expression of the HBZ gene of HTLV-1 correlates with proviral load, inflammatory markers and disease severity in HTLV-1 associated myelopathy/tropical spastic paraparesis (HAM/TSP). Retrovirology. 2009;6:19.
30. Pon JR, Wong J, Saberi S, Alder O, Moksa M, Grace Cheng SW, et al. MEF2B mutations in non-Hodgkin lymphoma dysregulate cell migration by decreasing MEF2B target gene activation. Nat Commun. 2015;6:7953.
31. Cosenza M, Pozzi S. The Therapeutic Strategy of HDAC6 Inhibitors in Lymphoproliferative Disease. Int J Mol Sci. 2018;19(8).
32. Di Giorgio E, Gagliostro E, Brancolini C. Selective class IIa HDAC inhibitors: myth or reality. Cell Mol Life Sci. 2015;72(1):73-86.
33. Xiong C, Guan Y, Zhou X, Liu L, Zhuang MA, Zhang W, et al. Selective inhibition of class IIa histone deacetylases alleviates renal fibrosis. FASEB J. 2019;33(7):8249-62.
34. Davis FJ, Gupta M, Camoretti-Mercado B, Schwartz RJ, Gupta MP. Calcium/calmodulin-dependent protein kinase activates serum response factor transcription activity by its dissociation

from histone deacetylase, HDAC4. Implications in cardiac muscle gene regulation during hypertrophy. J Biol Chem. 2003;278(22):20047-58.
35. Zhang M, Urabe G, Little C, Wang B, Kent AM, Huang Y, et al. HDAC6 Regulates the MRTF-A/SRF Axis and Vascular Smooth Muscle Cell Plasticity. JACC Basic Transl Sci. 2018;3(6):782-95.
36. Ye BH, Chung E, Pradhan K, Acuna-Villaorduna A, Wang Y, Shastri A, et al. S-Phase Progression of North American ATLL Cells Is Critically Regulated By the Proto-Oncogene BCL6 and Targetable By PARP Inhibition. Blood. 2019;134(Supplement_1):3779-.
37. Grant C, Nonnemacher M, Jain P, Pandya D, Irish B, Williams SC, et al. CCAAT/enhancer-binding proteins modulate human T cell leukemia virus type 1 long terminal repeat activation. Virology. 2006;348(2):354-69.
38. Yao J, Grant C, Harhaj E, Nonnemacher M, Alefantis T, Martin J, et al. Regulation of human T-cell leukemia virus type 1 gene expression by Sp1 and Sp3 interaction with TRE-1 repeat III. DNA Cell Biol. 2006;25(5):262-76.
39. Lehmann LH, Jebessa ZH, Kreusser MM, Horsch A, He T, Kronlage M, et al. A proteolytic fragment of histone deacetylase 4 protects the heart from failure by regulating the hexosamine biosynthetic pathway. Nat Med. 2018;24(1):62-72.
40. Lemasson I, Polakowski NJ, Laybourn PJ, Nyborg JK. Transcription regulatory complexes bind the human T-cell leukemia virus 5' and 3' long terminal repeats to control gene expression. Mol Cell Biol. 2004;24(14):6117-26.
41. Clerc I, Polakowski N, Andre-Arpin C, Cook P, Barbeau B, Mesnard JM, et al. An interaction between the human T cell leukemia virus type 1 basic leucine zipper factor (HBZ) and the KIX domain of p300/CBP contributes to the down-regulation of tax-dependent viral transcription by HBZ. J Biol Chem. 2008;283(35):23903-13.
42. Borowiak M, Kuhlmann AS, Girard S, Gazzolo L, Mesnard JM, Jalinot P, et al. HTLV-1 bZIP factor impedes the menin tumor suppressor and upregulates JunD-mediated transcription of the hTERT gene. Carcinogenesis. 2013;34(11):2664-72.
43. Mahgoub M, Yasunaga JI, Iwami S, Nakaoka S, Koizumi Y, Shimura K, et al. Sporadic on/off switching of HTLV-1 Tax expression is crucial to maintain the whole population of virus-induced leukemic cells. Proc Natl Acad Sci U S A. 2018;115(6):E1269-E78.
44. Meissner ME, Mendonca LM, Zhang W, Mansky LM. Polymorphic Nature of Human T-Cell Leukemia Virus Type 1 Particle Cores as Revealed through Characterization of a Chronically Infected Cell Line. J Virol. 2017;91(16).
45. Akari H, Fukumori T, Adachi A. Cell-dependent requirement of human immunodeficiency virus type 1 gp41 cytoplasmic tail for Env incorporation into virions. J Virol. 2000;74(10):4891-3.
46. Clocchiatti A, Di Giorgio E, Viviani G, Streuli C, Sgorbissa A, Picco R, et al. The MEF2-HDAC axis controls proliferation of mammary epithelial cells and acini formation in vitro. J Cell Sci. 2015;128(21):3961-76.
47. Azran I, Schavinsky-Khrapunsky Y, Aboud M. Role of Tax protein in human T-cell leukemia virus type-I leukemogenicity. Retrovirology. 2004;1:20.
48. Xie L, Yamamoto B, Haoudi A, Semmes OJ, Green PL. PDZ binding motif of HTLV-1 Tax promotes virus-mediated T-cell proliferation in vitro and persistence in vivo. Blood. 2006;107(5):1980-8.

49. Hivin P, Arpin-Andre C, Clerc I, Barbeau B, Mesnard JM. A modified version of a Fos-associated cluster in HBZ affects Jun transcriptional potency. Nucleic Acids Res. 2006;34(9):2761-72.
50. Thebault S, Basbous J, Hivin P, Devaux C, Mesnard JM. HBZ interacts with JunD and stimulates its transcriptional activity. FEBS Lett. 2004;562(1-3):165-70.
51. Yang YJ, Song TY, Park J, Lee J, Lim J, Jang H, et al. Menin mediates epigenetic regulation via histone H3 lysine 9 methylation. Cell Death Dis. 2013;4:e583.
52. Thakker RV. Multiple endocrine neoplasia type 1 (MEN1) and type 4 (MEN4). Mol Cell Endocrinol. 2014;386(1-2):2-15.
53. Halin M, Douceron E, Clerc I, Journo C, Ko NL, Landry S, et al. Human T-cell leukemia virus type 2 produces a spliced antisense transcript encoding a protein that lacks a classic bZIP domain but still inhibits Tax2-mediated transcription. Blood. 2009;114(12):2427-38.
54. Kuhlmann AS, Villaudy J, Gazzolo L, Castellazzi M, Mesnard JM, Duc Dodon M. HTLV-1 HBZ cooperates with JunD to enhance transcription of the human telomerase reverse transcriptase gene (hTERT). Retrovirology. 2007;4:92.
55. Matsumoto J, Ohshima T, Isono O, Shimotohno K. HTLV-1 HBZ suppresses AP-1 activity by impairing both the DNA-binding ability and the stability of c-Jun protein. Oncogene. 2005;24(6):1001-10.
56. Shah UA, Shah N, Qiao B, Acuna-Villaorduna A, Pradhan K, Adrianzen Herrera D, et al. Epidemiology and survival trend of adult T-cell leukemia/lymphoma in the United States. Cancer. 2020;126(3):567-74.
57. Costa EA, Magri MC, Caterino-de-Araujo A. The best algorithm to confirm the diagnosis of HTLV-1 and HTLV-2 in at-risk individuals from Sao Paulo, Brazil. J Virol Methods. 2011;173(2):280-6.
58. Haertle T, Carrera CJ, Wasson DB, Sowers LC, Richman DD, Carson DA. Metabolism and anti-human immunodeficiency virus-1 activity of 2-halo-2',3'-dideoxyadenosine derivatives. J Biol Chem. 1988;263(12):5870-5.
59. Harada S, Koyanagi Y, Yamamoto N. Infection of HTLV-III/LAV in HTLV-I-carrying cells MT-2 and MT-4 and application in a plaque assay. Science. 1985;229(4713):563-6.
60. Posch W, Piper S, Lindhorst T, Werner B, Fletcher A, Bock H, et al. Inhibition of human immunodeficiency virus replication by cell membrane-crossing oligomers. Mol Med. 2012;18:111-22.
61. Rowe T, Dezzutti C, Guenthner PC, Lam L, Hodge T, Lairmore MD, et al. Characterization of a HTLV-I-infected cell line derived from a patient with adult T-cell leukemia with stable co-expression of CD4 and CD8. Leuk Res. 1995;19(9):621-8.
62. Arnold J, Zimmerman B, Li M, Lairmore MD, Green PL. Human T-cell leukemia virus type-1 antisense-encoded gene, Hbz, promotes T-lymphocyte proliferation. Blood. 2008;112(9):3788-97.
63. Feuer G, Fraser JK, Zack JA, Lee F, Feuer R, Chen IS. Human T-cell leukemia virus infection of human hematopoietic progenitor cells: maintenance of virus infection during differentiation in vitro and in vivo. J Virol. 1996;70(6):4038-44.
64. Koeffler HP, Chen IS, Golde DW. Characterization of a novel HTLV-infected cell line. Blood. 1984;64(2):482-90.
65. Panfil AR, Al-Saleem J, Howard CM, Mates JM, Kwiek JJ, Baiocchi RA, et al. PRMT5 Is Upregulated in HTLV-1-Mediated T-Cell Transformation and Selective Inhibition Alters Viral Gene Expression and Infected Cell Survival. Viruses. 2015;8(1).

66. Maeda M. Human T lymphotropic virus type-I (HTLV-I) immortalizes human T cells in vitro--its implication in the pathogenesis of adult T cell leukemia (ATL). Hum Cell. 1992;5(1):70-8.
67. Ahsan MK, Masutani H, Yamaguchi Y, Kim YC, Nosaka K, Matsuoka M, et al. Loss of interleukin-2-dependency in HTLV-I-infected T cells on gene silencing of thioredoxin-binding protein-2. Oncogene. 2006;25(15):2181-91.
68. Lavorgna A, Matsuoka M, Harhaj EW. A critical role for IL-17RB signaling in HTLV-1 tax-induced NF-kappaB activation and T-cell transformation. PLoS pathogens. 2014;10(10):e1004418.
69. Choi YB, Harhaj EW. HTLV-1 tax stabilizes MCL-1 via TRAF6-dependent K63-linked polyubiquitination to promote cell survival and transformation. PLoS pathogens. 2014;10(10):e1004458.
70. Tateno M, Kondo N, Itoh T, Chubachi T, Togashi T, Yoshiki T. Rat lymphoid cell lines with human T cell leukemia virus production. I. Biological and serological characterization. J Exp Med. 1984;159(4):1105-16.

919

Figures

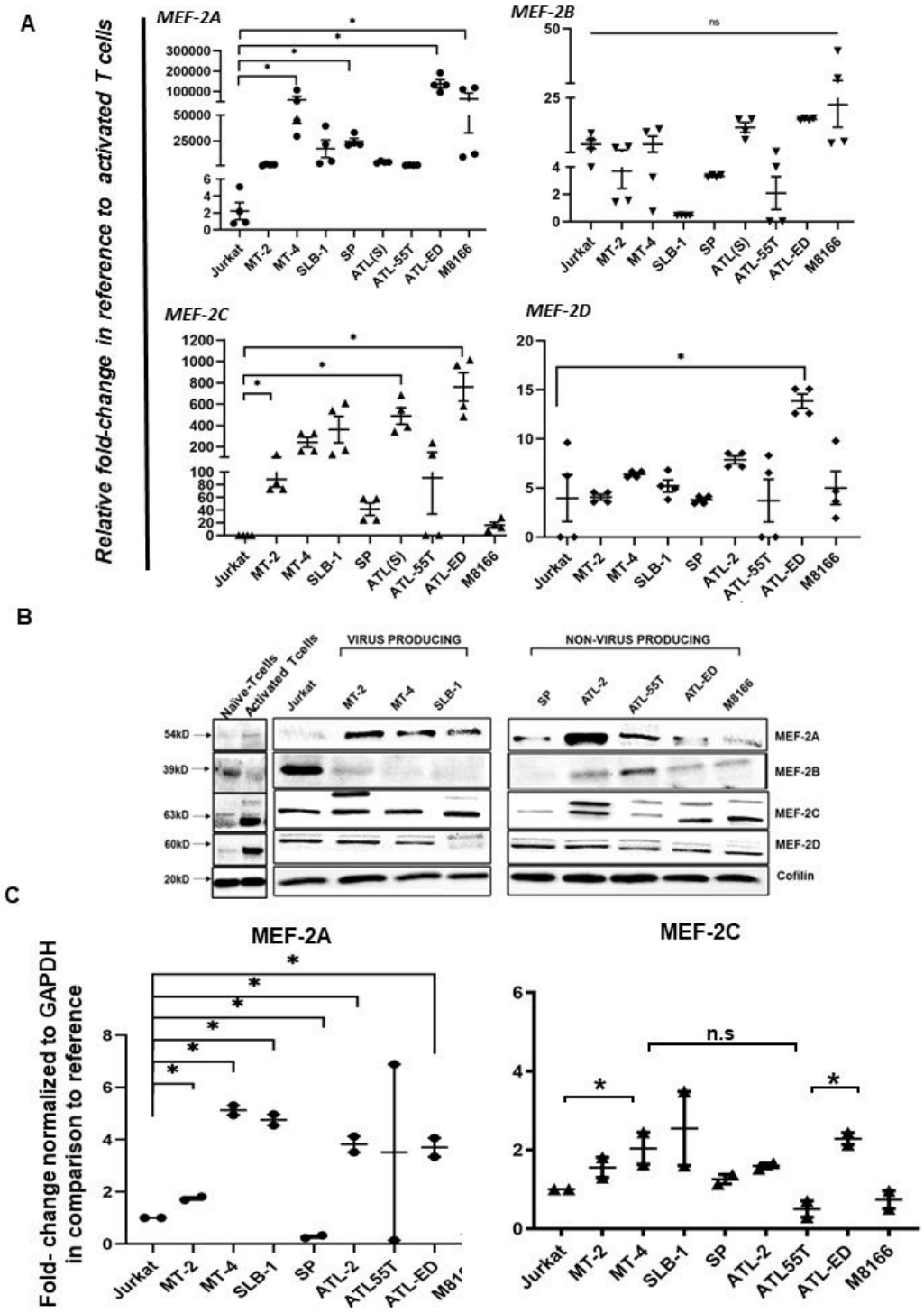

Figure 1

(figure caption not included)

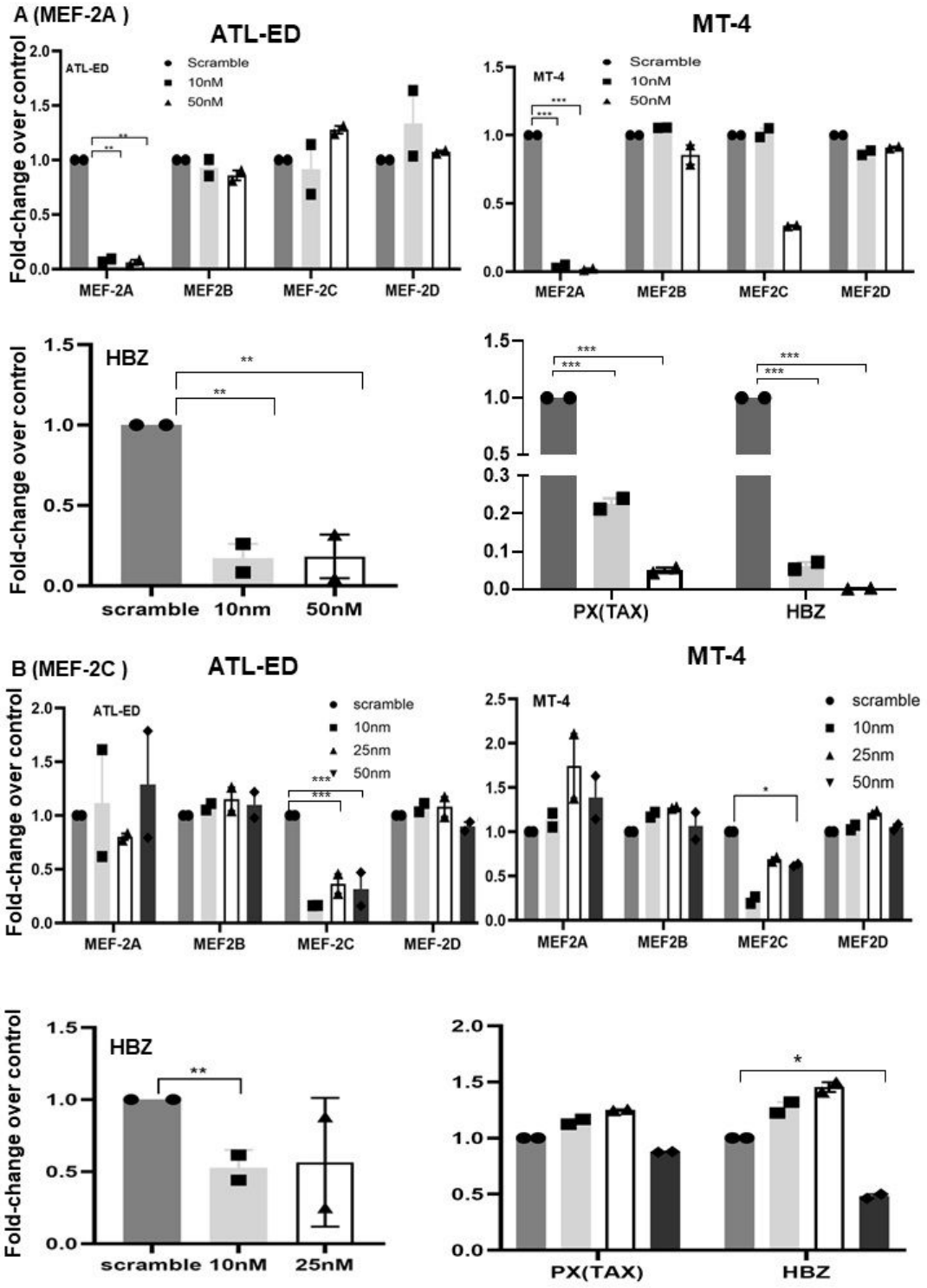

Figure 2

(figure caption not included)

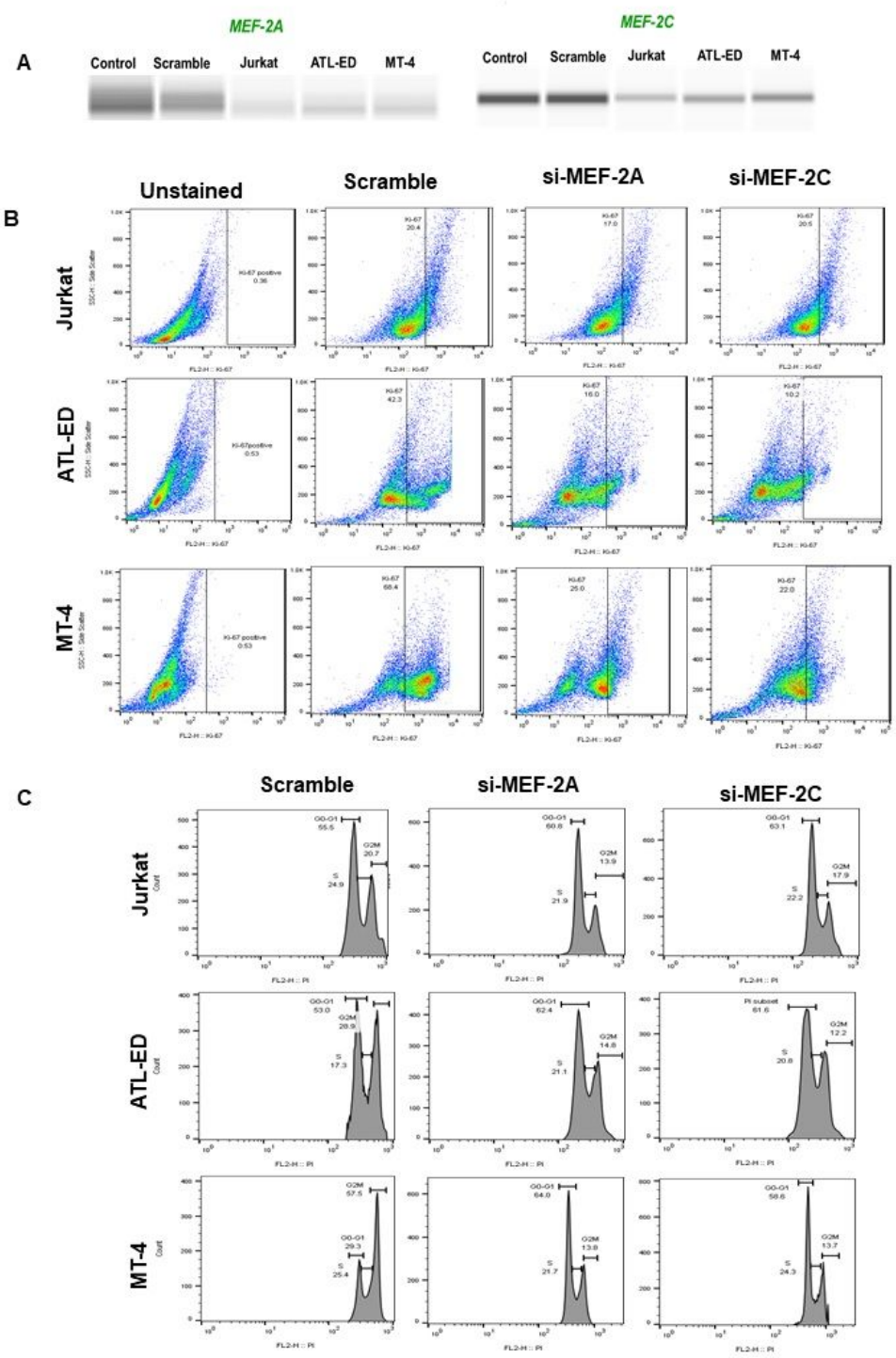

Figure 3

(figure caption not included)

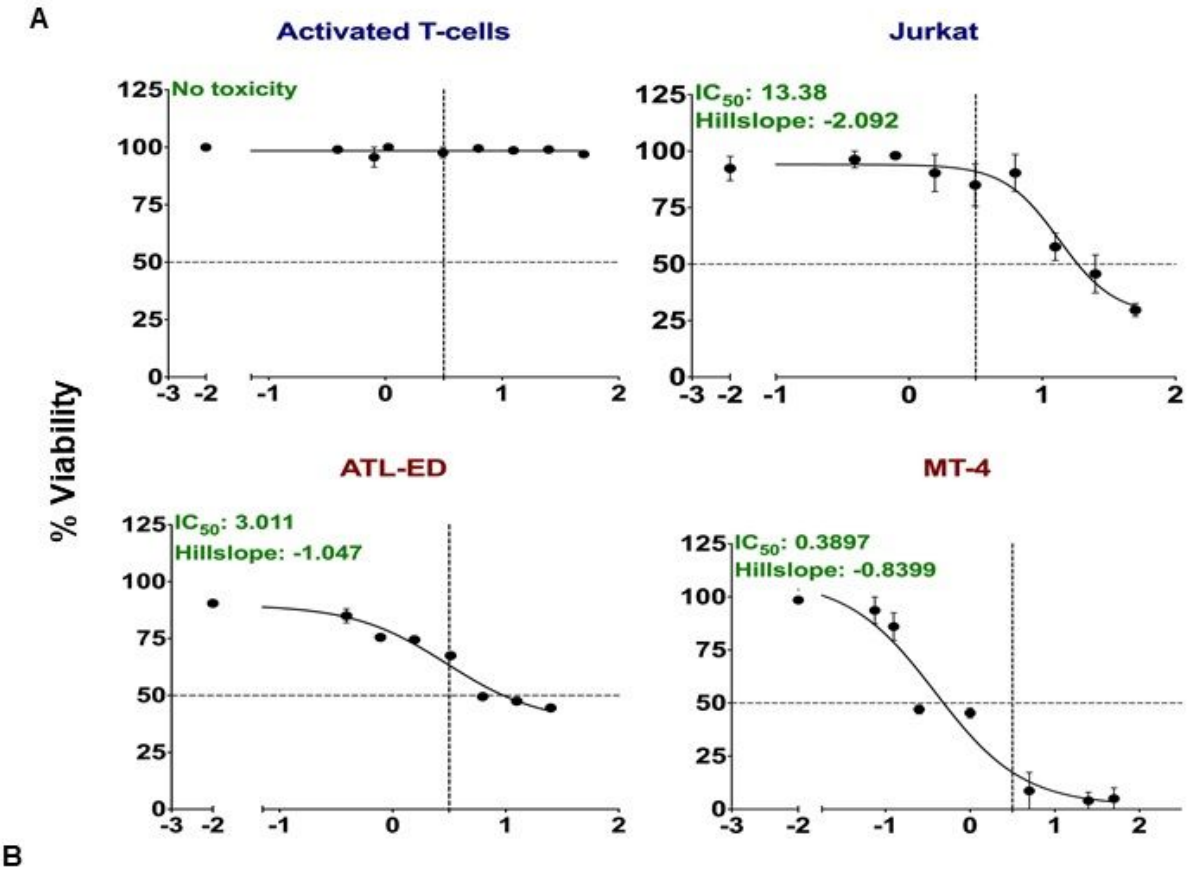

Cell lines	MC1568 IC50 (uM, hillslope)					
	w/o siRNA	siSRF	siMEF-2A	siMEF-2C	TAX (overexpression)	HBZ (overexpression)
Jurkat	13.38 (-2.0)	14.74 (-1.6)	No toxicity	No toxicity	15.71 (-0.95)	20.20 (-1.024)
MT-4	0.38 (-0.83)	0.69 (-2.9)	20.96 (-0.6)	No toxicity	2.65 (-0.76)	1.324 (-10.78)
ATL-ED	3.02 (-1.0)	3.34 (-1.5)	25.68 (-5.8)	No toxicity	16.65 (-0.52)	11.70 (-0.5)

Figure 4

(figure caption not included)

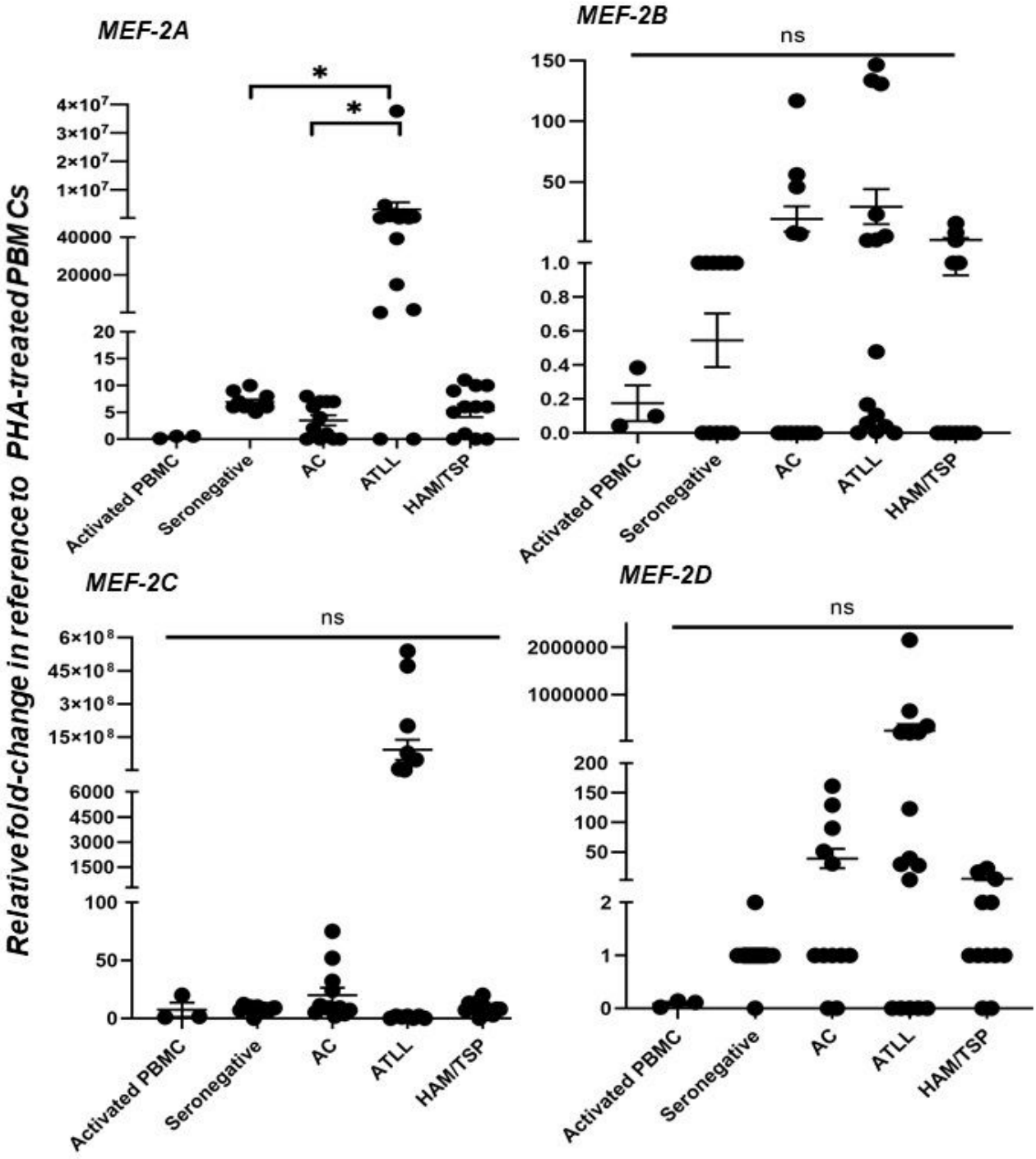

Figure 5

(figure caption not included)

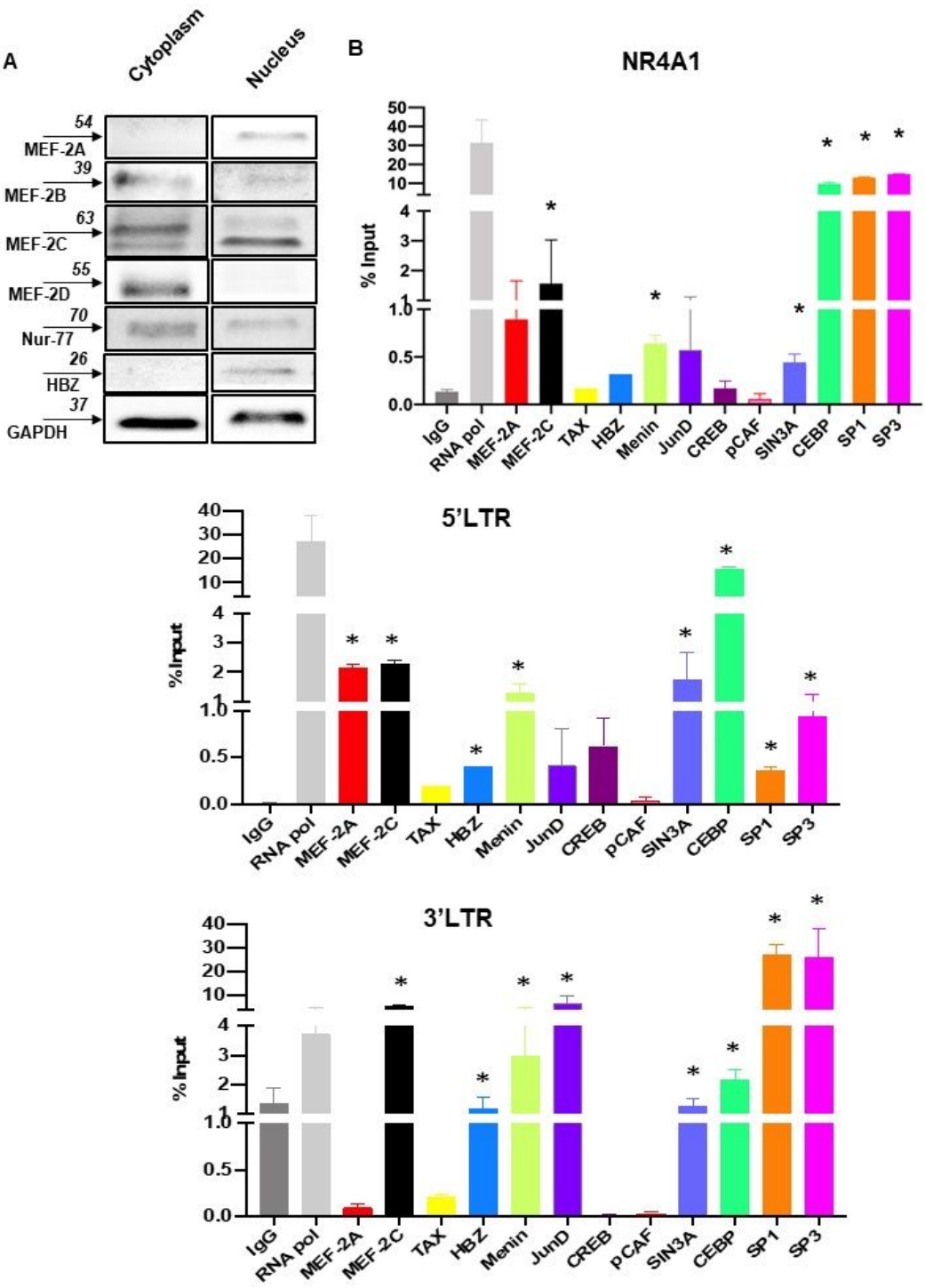

Figure 6

(figure caption not included)

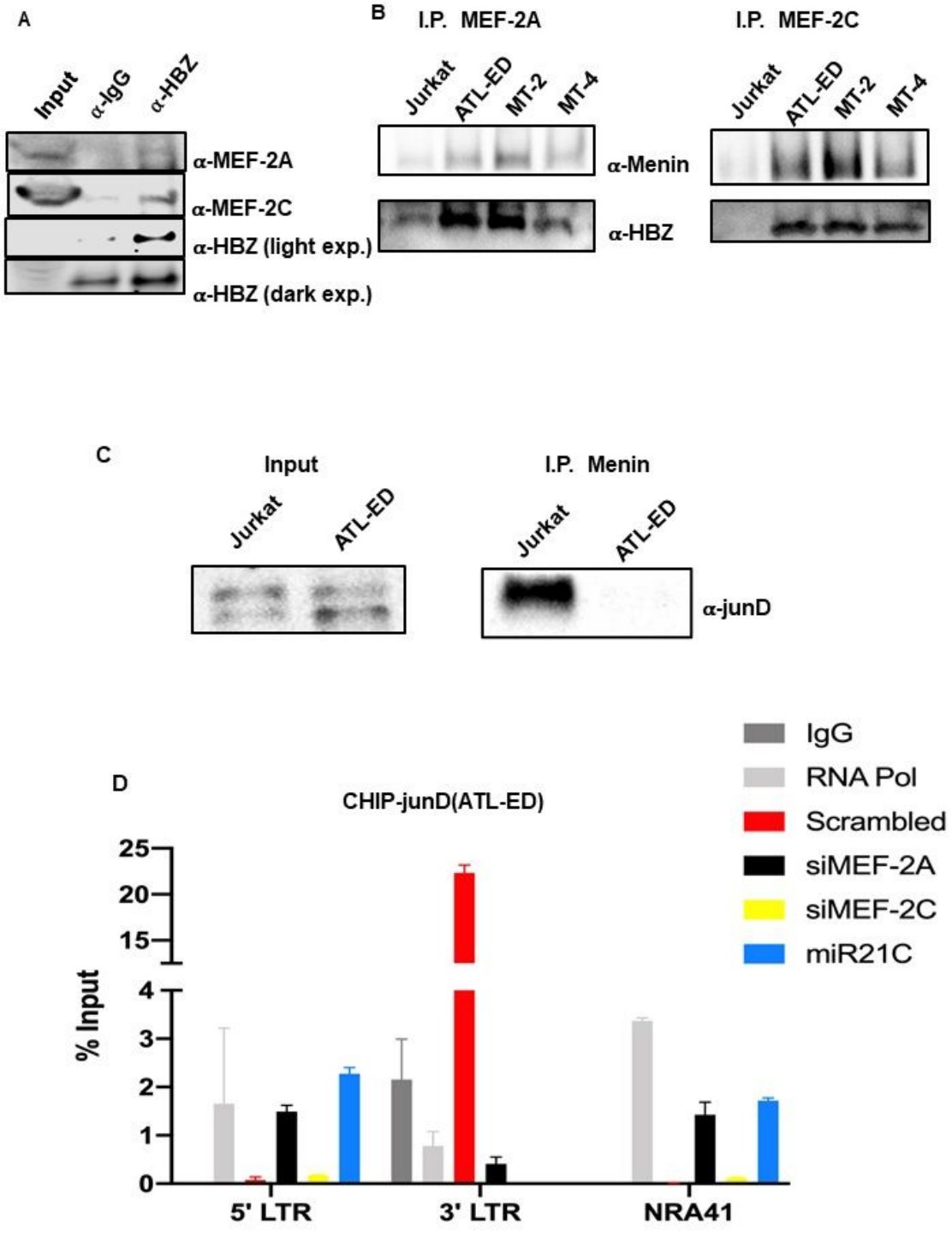

Figure 7

(figure caption not included)

Supplementary Files

This is a list of supplementary files associated with this preprint. Click to download.

- Fig.S1.png
- Fig.S2.png
- Fig.S3.png
- Fig.S4.png
- SupplementaryTables.docx